

LASER APPLICATIONS AND OTHER TOPICS IN QUANTUM ELECTRONICS https://doi.org/10.1070/QEL17972

Laser synthesis of nanocomposite hydrocarbon fuel and CARS diagnostics of its combustion flame

E.V. Barmina, V.D. Kobtsev, S.A. Kostritsa, S.N. Orlov, V.V. Smirnov, M.I. Zhilnikova, O.V. Uvarov, G.A. Shafeev

Abstract. **We report an analysis of diffusive combustion in oxygen of a composite fuel formed by the addition of aluminium nanoparticles (NPs) to isopropanol. The process of obtaining Al NPs consisted in laser fragmentation of initially large industrial NPs using radiation of a pulsed nanosecond neodymium laser. The size distribution of Al NPs was determined using a measuring disk centrifuge. The average nanoparticle size was 20 nm, which is confirmed by transmission electron microscopy data. A diagnostic system based on coherent anti-Stokes Raman scattering (CARS) was used to experimentally study the diffusive combustion of composite fuel. The temperature distributions were measured in two mutually orthogonal directions (along the flame and in the transverse direction) in pure isopropanol and in isopropanol with the addition of 0.15 wt% of Al nanoparticles.**

Keywords: *hydrocarbons and composite fuels, laser fragmentation, aluminium nanoparticles.*

1. Introduction

Nanoparticles of metals such as aluminium have a high calorific value and generate more energy per unit volume. The properties of hydrocarbon fuels with additives of partially oxidised aluminium nanoparticles (NPs) were studied in [1, 2]. Experiments on the combustion of a suspension of Al NPs 50 nm in size in biofuel (ethanol) were carried out in [1]. It was found that the volume fraction of Al NPs in the range of 1%–3% does not affect the heat release during combustion.

An important aspect in the experimental study of the combustion processes of fuels containing hydrocarbons and metal components is the use of modern contactless methods and systems for diagnosing the parameters and composition of the combustion products of these fuels. These methods include spectroscopy based on coherent anti-Stokes Raman scattering (CARS) [3].

The main goal of this work is to obtain comparative information about the temperature distributions in the flame during the combustion of isopropanol [$CH_3CH(OH)CH_3$] and isopropanol with aluminum NPs in an oxygen atmosphere. Such measurements make it possible to directly characterise the combustion process (especially heat release properties) of its spatial structure in different zones of the flame. In addition, these data will make it possible to verify the proposed theoretical combustion models and evaluate the efficiency of using composite fuels in practical applications.

Smirnov et al. [4] used aluminium NPs free from the surface oxide film as an additive to n-decane ($C_{10}H_{22}$). The NPs were obtained by the plasma decomposition of triethylaluminium in the absence of oxygen, followed by rapid cooling of the decomposition products with liquid hydrocarbon fuel. It was found that in the diffusive combustion of n-decane with aluminium NPs with a fraction of 2.5 wt%, the temperature in the flame front at a certain cut from the burner nozzle is 300–400 K higher than that in the flame of pure n-decane. This difference was explained by the higher combustion rate of fuel with Al NPs. At large distances, where complete combustion of both types of fuel occurs, the observed difference in temperatures decreases to 90°C and characterises an increase in the calorific value of decane with additions of Al.

An alternative method for the synthesis of aluminium NPs is laser ablation of an Al target in liquid hydrocarbons [5]. Aluminium nanoparticles obtained by this method are covered with a 2–3-nm thick layer of natural oxide.

Another possibility of obtaining small-size aluminium NPs is the process of laser fragmentation of Al powders with initial sizes in the range from several micrometres to hundreds of nanometres. This process is well known and applicable to a wide class of materials [6–10]. In this case, there is no massive target, and fragmentation (reduction in size) occurs due to the interaction of laser radiation with individual particles, which, being in the waist of the laser beam, melt and split into smaller fragments due to hydrodynamic interaction with vapours of the surrounding liquid being at high pressure.

In our previous work [11], we demonstrated laser fragmentation of aluminium NPs with an initial size from 100 to 600 nm and with a distribution maximum near 400 nm, obtained by explosion of aluminium wires in vacuum. (Such NPs produced by LLC Advanced Powder Technologies are referred to as ALEX.) Isopropyl alcohol was used as a medium for fragmentation of Al NPs. After sedimentation of the colloidal solution under the action of gravity for several days, the excess alcohol was removed, and the concentrate of aluminium NPs was added to n-decane to obtain initial samples of composite fuels. Fragmentation of the initial Al NPs was carried out in liquid isopropanol using radiation from an ytterbium-doped fibre laser with a pulse energy of 1 mJ, a pulse duration of 100 ns, and a pulse repetition rate of 20 kHz. After fragmentation, a significant part of the nanoparticles still had a size of more than 100 nm, which excluded the possibility of the formation of their stable colloidal solution in liquid.

In this work, when obtaining the final product (a mixture of aluminium NPs with hydrocarbon fuel), the stage of substitution of isopropyl alcohol for n-decane was excluded. The

E.V. Barmina, V.D. Kobtsev, S.A. Kostritsa, S.N. Orlov, V.V. Smirnov, M.I. Zhilnikova, O.V. Uvarov, G.A. Shafeev Prokhorov General Physics Institute of the Russian Academy of Sciences, ul. Vavilova 38, 119991 Moscow, Russia; e-mail: barminaev@gmail.com

Received 30 September 2021
Kvantovaya Elektronika **52** (1) 100–104 (2022)
Translated by I.A. Ulitkin

final fuel was a mixture of isopropyl alcohol with Al nanoparticles, to reduce the size of which the initial nanopowder was fragmented using a laser source of higher intensity. The obtained colloidal solution of isopropyl alcohol with Al NPs was tested in a diffusive-type burner. High purity oxygen was used as an oxidising agent. Temperature measurements were carried out using CARS spectroscopy of nitrogen molecules in various flame sections during the combustion of both pure isopropanol and isopropanol with the addition of aluminium NPs.

2. Experiment and discussion of results

2.1. Laser fragmentation of aluminium nanoparticles

For fragmentation of the initial Al nanoparticles, we used a neodymium laser with a pulse energy of 2 mJ, a pulse duration of 10 ns, and a repetition rate of 10 kHz. Compared to [11], in these experiments, the peak intensity of laser radiation was 20 times higher than that of an ytterbium-doped fibre laser. This made it possible to reduce the time of laser fragmentation of the initial NPs and to decrease their size. The details of the experiment are described in [11]. Laser radiation was focused into a suspension of initial Al NPs in isopropanol from bottom to top through a window transparent for laser radiation. The typical volume of the suspension was 5 mL. Before and during irradiation, the liquid was purged with molecular hydrogen to displace other dissolved gases. The cell with the suspension was cooled with running water. The size distribution of nanoparticles was determined using a CPS-2000 disk measuring centrifuge. The morphology of Al NPs was studied using a Carl Zeiss transmission electron microscope (TEM) with an accelerating voltage of 200 kV.

The laser fragmentation time was determined empirically. The fragmentation process depends on a parameter equal to the ratio of the effective volume of the laser beam in the medium to the total volume of the suspension. As a rule, this value is about 10^{-3}. For fragmentation, it is necessary that most nanoparticles in the suspension be in the waist of the laser beam at least once. The final size distribution of NPs is bimodal, since the dominant fragmentation mechanism is the separation of small particles from large ones [10]. With an increase in the fragmentation time, all large particles are fragmented into smaller ones.

The distributions of the mass and number of NPs by size in a sample with a volume of 100 μL are shown in Fig. 1. The largest number of nanoparticles has a diameter of less than 10 nm. Such NPs are not subject to sedimentation under natural gravity, and the resulting colloidal solution remains stable for at least several days. Note that, in contrast to [11], there are no large nanoparticles with sizes of 300–500 nm in the sample.

A TEM image of fragmented aluminium NPs is shown in Fig. 2. It can be seen that the particles are mostly spherical. Figure 3 shows an image of Al NPs obtained in scattered electrons with a high magnification; the internal structure of nanoparticles is visible.

It should be noted that there are cavities in the central regions of some NPs. This morphology of Al nanoparticles was also observed earlier in other works on laser ablation of aluminium in ethanol with the formation of larger NPs (see, for example, [12]). Presumably, these cavities are filled with hydrogen. This can be explained as follows. At the initial stage of laser fragmentation, the separated nanoparticle is in a liquid state, and the solubility of H_2 in liquid aluminium is an

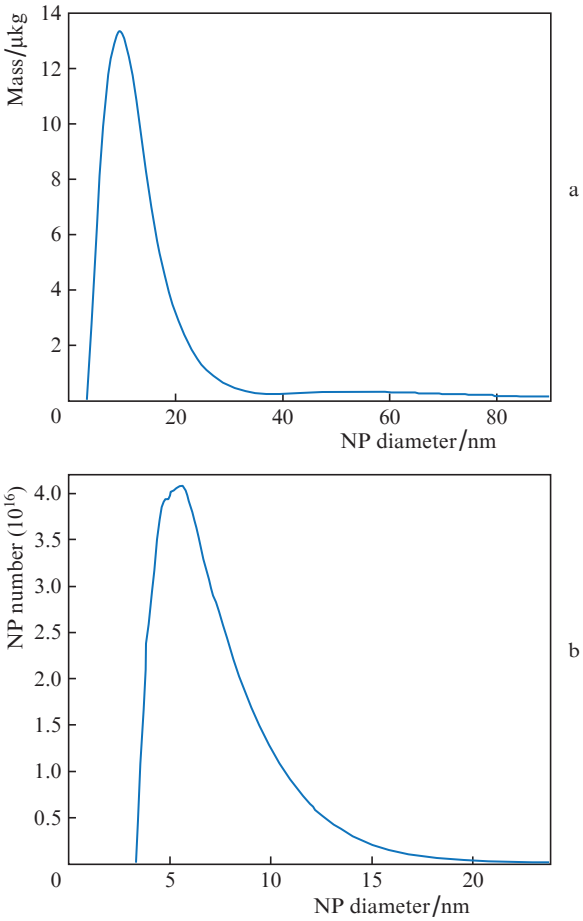

Figure 1. Size distributions of (a) mass and (b) number of Al NPs in a sample with a volume of 100 μL. Laser fragmentation time is 40 min.

order of magnitude higher than that in solid aluminum. Consequently, the hydrogen dissolved in the liquid Al NP after its solidification turns out to be supersaturated and remains in the metal shell [12]. Note also that, in addition to hydrogen,

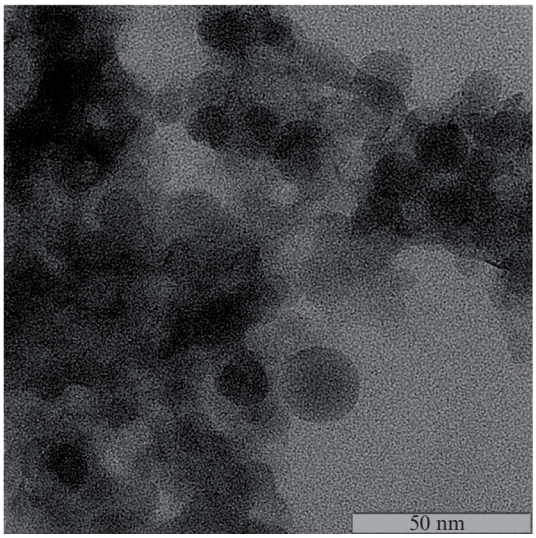

Figure 2. TEM image of a suspension of Al nanoparticles after laser fragmentation.

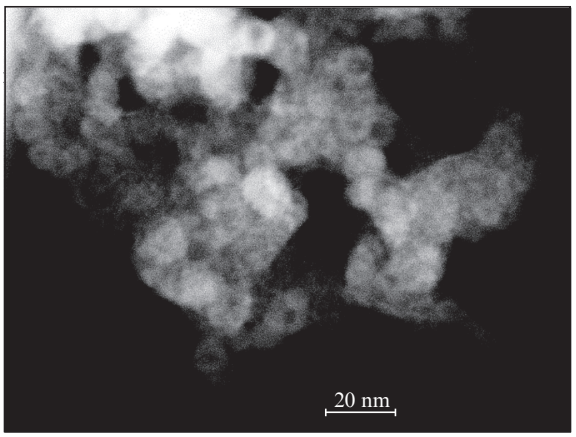

Figure 3. Scattered transmission electron microscopy (STEM) image of fragmented Al NPs.

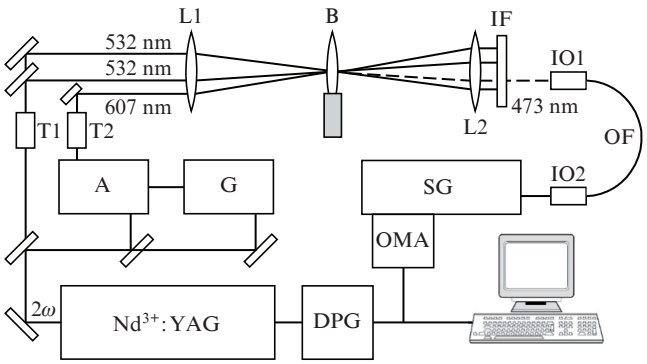

Figure 4. Scheme of a CARS spectrometer: (Nd^{3+}:YAG) pump YAG laser (second harmonic); (G and A) dye laser generator and amplifier; (T1 and T2) telescopes; (L1 and L2) focusing and collimating lenses; (B) burner; (IF) narrow-band interference filter; (IO1 and IO2) radiation input and output devices; (OF) optical fibre; (SG) spectrograph; (OMA) optical multichannel analyser; (DPG) delayed pulse generator.

which is forcibly blown through the cell with the suspension, there is an additional source of hydrogen generation associated with the decomposition of alcohol under the action of laser breakdown [13].

2.2. Burner

To study the combustion process of liquid hydrocarbon fuels with additives of Al NPs, we designed a stand consisting of a burner with a diffusive type of fuel and oxidiser mixing [4] and a diagnostic system based on CARS spectroscopy. This type of burner makes it possible to obtain stable laminar flames with a stationary, well-defined geometry of the flame front, which, in turn, allows one with sufficient accuracy to record changes in flame parameters during the combustion of both a pure fuel and a combined fuel containing metal NPs.

The choice of the burner design is due to the need to prepare a vapour–gas mixture of fuel with nanoparticles. Taking into account the high oxidising ability of Al NPs, the process of atomisation and evaporation must be separated from the process of mixing the fuel mixture with an oxidising agent. To deliver the vapour mixture into the mixing zone, use is made of an inert gas, nitrogen in this case, which flows from the flow control and regulation system to the fuel injector. Fuel, isopropanol in this case, is supplied to the injector via a capillary fuel line from a precision metering system based on a syringe pump. This system provides a regulated fuel supply at a rate from 2 to 150 mL h^{-1}.

2.3. CARS diagnostic system

To study the spatial distribution of the flame temperature, the burner was placed on a three-coordinate translation stage, which made it possible to move the flame front relative to the laser beams of the CARS spectrometer (Fig. 4) with a positioning accuracy of ± 10 μm. The experimental complex for measuring the distribution of local values of temperatures in the flame includes a burner with the supply and control of fuel and oxidiser flows, as well as a CARS laser diagnostic system with an appropriate system for monitoring and controlling radiation parameters.

The values measured by CARS thermometry are limited from above by the temperatures at which molecules selected as reference points (in this case, N_2 molecules) are dissociated, and lie in the range of 3500–4000 K. Measurements showed that the relative random measurement error is 3.6%. This value characterises the temperature measurement error in a time equal to the duration of a single laser pulse (~10 ns). With an increase in the measurement time to 1 s (averaging over 10 laser pulses with a repetition rate of 10 Hz), the relative random error decreases to 1.2%. In this case, the relative systematic error was 0.5%.

The spatial resolution in this experiment was determined by the volume of interaction of the beams in the region of their focusing, which can be characterised by the confocal parameter b and the transverse size of the intersection of the beams $2\omega_0$. In the experiment, when focusing beams with a lens with a focal length of 200 mm, $b \times 2\omega_0 = 2 \times 0.2$ mm^2. The lasing line width of the dye laser was 200 cm^{-1}. The temperature was determined by minimising the mismatch between the experimental and calculated CARS spectra with varying the parameters of the calculated spectrum, the main of which is temperature. A typical CARS spectrum of nitrogen mole-

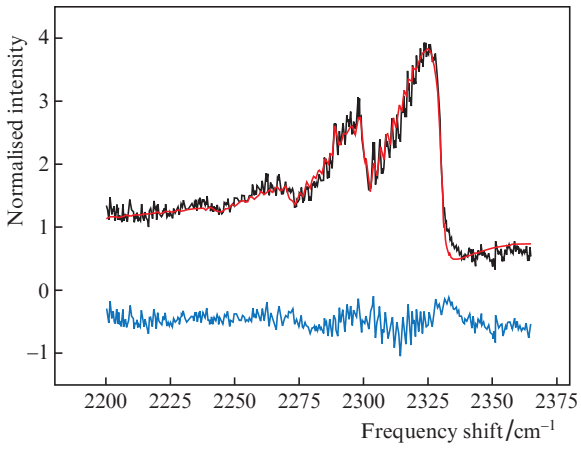

Figure 5. (Colour online) CARS spectra of N_2 molecules in the flame of a colloidal solution of isopropyl alcohol with Al NPs corresponding to a temperature of 1905 K [black curve = experiment, red curve = theory, blue curve = difference between the calculated and experimental spectra (shifted relative to zero)].

cules in a flame and the result of this 'fit' are shown in Fig. 5. A schematic of the relative position of the flame and laser beams of the diagnostic system is shown in Fig. 6.

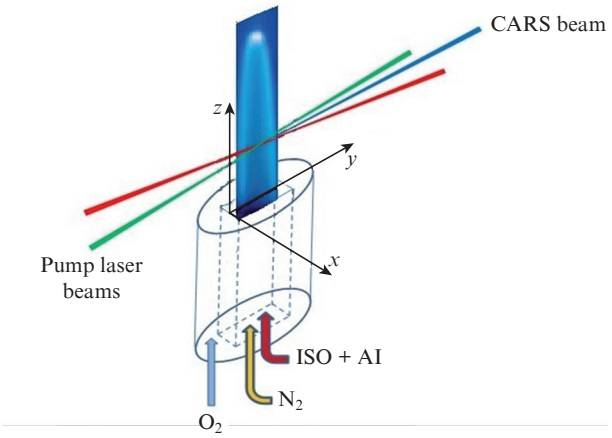

Figure 6. (Colour online) Relative position of the burner, flame and laser beams of the CARS spectrometer (the origin lies in the plane of the burner nozzle). The dashed lines show the internal heated volume, which serves for the formation of a nitrogen-containing vapour–gas mixture of isopropyl alcohol (ISO) with Al NPs.

2.4. Measurement of the distribution of the relative concentrations of fuel, oxidiser and temperature in the flame

To analyse the process of mixing a vapour–gas mixture (alcohol-based fuel + nitrogen carrier gas) with oxygen (in a cocurrent flow) as a result of their mutual diffusion, we studied the profiles of nitrogen and oxygen concentrations. Since the vapour–gas mixture of fuel with nitrogen, produced in the burner evaporator before mixing with the oxidiser, is uniformly mixed, the spatial distribution of nitrogen molecules should correspond to the distribution of fuel molecules.

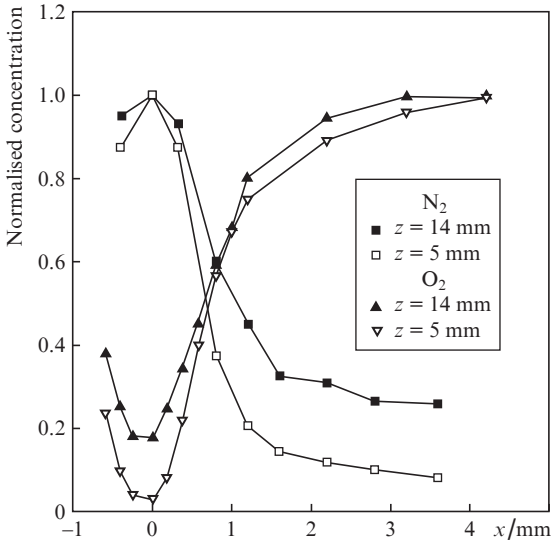

Figure 7. Profiles of the relative concentrations of nitrogen and oxygen molecules during their mutual diffusion in a cocurrent flow.

The results of measuring the relative concentrations of N_2 and O_2 molecules in a cold flow, presented in Fig. 7, show that the experiment allows one to obtain detailed information about the concentrations and their distribution in the mixing region of the fuel and oxidiser flows. Figure 7 shows that when measurement are performed in the direction perpendicular to the flow axis, there is a symmetry of the distributions of N_2 and O_2 concentrations relative to the flow axis; in addition, mutual diffusive penetration of the oxidant (O_2) into the jet of fuel and nitrogen (and, accordingly, the fuel into the jet of oxidiser) is observed as they move along the flow.

Next, we studied the diffusive combustion of a mixture of a synthesised combined fuel consisting of isopropyl alcohol and Al NPs (0.15 wt% of the initial isopropanol) with oxygen. Spatial temperature profiles were measured directly in the combustion zone during the combustion of pure isopropyl alcohol and alcohol with aluminium NPs. Figure 8 shows the temperature distributions recorded along the x axis at distances of 5 and 14 mm from the nozzle exit.

A comparative analysis is performed of the parameters of the reacting mixture during combustion of the fuel in the form of pure isopropyl alcohol and alcohol containing 0.15 wt% Al

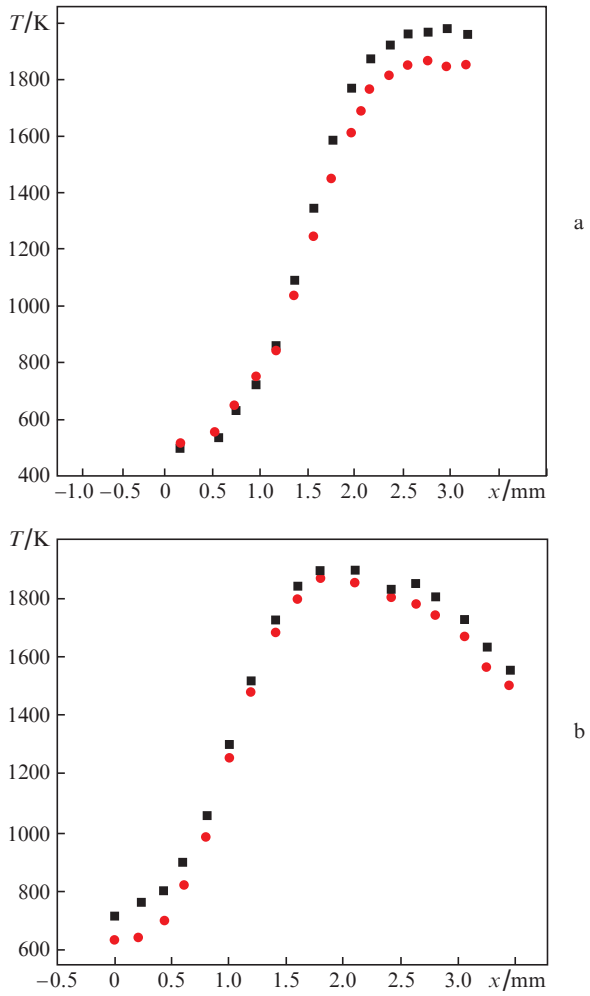

Figure 8. (Colour online) Temperature distributions along the x axis from the flow centre to the periphery in flames of pure isopropanol (red circles) and isopropanol with additives of Al NPs (black squares) at a distance z of (a) 5 and (b) 14 mm from the nozzle exit downstream. The content of aluminium nanoparticles is 0.15 wt%.

nanoparticles. The most characteristic features are as follows. In the case of fuel combustion with Al NPs, the temperature values are higher and repeat the temperature profile measured for pure alcohol. In the regions of the flame front, where the fuel and oxidiser are mixed, the temperature difference for the two types of fuel increases with increasing distance downstream and reaches its maximum value equal to 110 K at a distance $z = 5$ mm from the nozzle exit. In this case, the temperature during the combustion of pure alcohol is 1800–1850 K, and in the case of alcohol with Al NPs, the temperature reaches 1850–2000 K. The observed temperatures along the front downstream indicate a higher combustion rate of fuel with nanoparticles. With an increase in the distance from the nozzle exit by more than 5 mm, the temperature in the flow with pure alcohol continues to increase, while the temperature during the combustion of alcohol with Al NPs in the cross section near $z = 14$ mm stabilises and equals 2000 K, which indicates complete burnout of the fuel with nanoparticles at $z = 14$ mm. At a greater distance from the nozzle, the temperatures in the front of both flows stop increasing and their difference is 100 K, which is apparently associated with a higher specific heat release from the fuel with Al NPs. In this case, an increase in temperature is observed in the centre of the burner due to diffusive penetration of the oxidiser to the jet centre.

3. Conclusions

We have presented the results of investigations aimed at developing the synthesis of a composite fuel based on Al nanoparticles and isopropanol and studying the features of its combustion in a specially designed burner using laser diagnostics methods. A characteristic feature of the developed approach to the synthesis of nanoparticles is laser fragmentation of Al nanopowder directly in liquid hydrocarbon fuel. The use of a laser with a pulse energy of 2 mJ made it possible to significantly reduce the size of fragmented Al NPs down to 10–20 nm. (In this case, there are no larger particles.) The addition of such particles to isopropanol in fraction of only 0.15 wt% makes it possible to increase the flame temperature by 100–150 K in comparison with the temperature in the case of pure isopropanol.

The results of the measurements are supposed to be used to test the proposed theoretical models, simulate kinetic and dynamic processes in the flow of a reacting mixture, and evaluate the efficiency of using the developed composite fuels for practical applications.

It should be noted that the complexity of the combustion processes of nanoparticles, even in a flame of such a simple form, requires additional research to clarify the effect of evaporation of nanoparticles, secondary reactions, clustering of combustion products, etc.

Acknowledgements. This work was supported by the Russian Science Foundation (Grant No. 20-19-00419).

References

1. Allen C. et al. *Proc. Combustion Institute*, **33** (2), 3367 (2011).
2. Jones M., Li C.H., Afjeh A., et al. *Nanoscale Res. Lett.*, **6**, 246 (2011).
3. Greenhalgh D.A., in *Advances in Nonlinear Spectroscopy.* Ed. by R.J.H. Clark and R.E. Hester (Chichester: John Wiley & Sons, 1988) Vol.15, pp 193 – 251.
4. Smirnov V.V., Kostritsa S.A., Kobtsev V.D., Titova N.S., Starik A.M. *Combustion and Flame*, **162** (10), 3554 (2015).
5. Stratakis E., Barberoglou M., Fotakis C., Viau G., Garcia C., Shafeev G.A. *Opt. Express*, **17** (150), 12650 (2009).
6. Prochazka M. et. al. *Anal. Chem.*, **69**, 5103 (1997).
7. Ziefuss A.R. et al. *J. Phys. Chem. C*, **122**, 22125 (2018).
8. Delfour L. et al. *J. Phys. Chem. C*, **119**, 13893 (2015).
9. Pyatenko A. et al. *Laser Photonics Rev.*, **7** (4), 596 (2013).
10. Kuzmin P.G., Shafeev G.A., Serkov A.A., Kirichenko N.A., Shcherbina M.E. *Appl. Surf. Sci.*, **294**, 15 (2014).
11. Smirnov V.V., Zhilnikova M.I., Barmina E.V., Shafeev G.A., Kobtsev V.D., Kostritsa S.A., Pridvorova S.M. *Chem. Phys. Lett.*, **763** (2), 138211 (2021).
12. Viau G., Colliére V., Lacroix L.-M., Shafeev G.A. *Chem. Phys. Lett.*, **501**, 419 (2011).
13. Baymler I.V., Barmina E.V., Simakin A.V., Shafeev G.A. *Quantum Electron.*, **48** (8), 738 (2018) [*Kvantovaya Elektron.*, **48** (8), 738 (2018)].